This is a repository copy of *Nanocapsules of Sterculia striata acetylated polysaccharide as a potential monomeric amphotericin B delivery matrix*.

White Rose Research Online URL for this paper:
http://eprints.whiterose.ac.uk/143428/

Version: Accepted Version

Article:

Nanocapsules of Sterculia striata acetylated polysaccharide as a potential monomeric amphotericin B delivery matrix

Fernanda M. Sombra[a], Ana Rosa Richter[a], Alyne Rodrigues de Araujo[b], Fabio de Oliveira Silva Ribeiro[b], Durcilene Alves da Silva[b] Haroldo C.B. Paula[c], Judith P.A. Feitosa[a], Francisco. M. Goycoolea[d,e], Regina C.M. de Paula[a]*

[a] Departament of Organic and Inorganic Chemistry - UFC - CEP, Caixa Postal 6021 - Humberto Monte s/n, Campus do Pici, 60455-760 Fortaleza, Brazil.

[b]Nucleo de Pesquisa em Biodiversidade e Biotecnologia, BIOTEC, **Campus** Ministro Reis Velloso, Universidade Federal do Piaui,

[c] Department of Analytical and Physical Chemistry - UFC, Fortaleza, Brazil

[d] University of Munster, Institute of Plant Biology and Biotechnology, Schlossgarten 3, D-48149 Munster, Germany

[e] School of Food Science and Nutrition, University of Leeds, Leeds LS16 7PA, U.K.

ABSTRACT

Stable oil nanocapsules based on acetylated Sterculia striata polysaccharide (ASSP) were produced without the use of a surfactant, and derivatives of ASSP with four different degrees of substitution (DS) were synthesised. The data revealed that only derivatives with high DS were able to produce nanocapsules (NC), which exhibited monomodal size distribution profiles with a Z-average particle size, ζ-potential, and polydispersity index (PDI) that were dependent on ASSP DS and concentration. Nanocapsules were loaded with amphotericin B (AMB) with encapsulation efficiencies (EE%) thatwere dependent on drug and ASSP concentrations and DS. A maximum EE% value of 99.2%was achieved, and the loaded AMBwas found to be in amonomeric form, evenwith a concentration one hundredfold higher than that usually observed for commercial AMB aqueous solutions. Loaded nanocapsules show an in vitro controlled release of AMB. As the monomeric AMB state decreased drug toxicity, ASSP nanocapsules loaded with AMB (NC1.68) have potential for use as a drug delivery system. AMB loaded NC 1.68 keeps its activity against 5 strains of Candida albicans tested.

Corresponding author: Regina Celia Monteiro de Paula rpuala@dqoi.ufc.br

Departament of Organic and Inorganic Chemistry - UFC - CEP, Caixa Postal 6021 - Humberto Monte s/n, Campus do Pici, 60455-760 Fortaleza, Brazil.

1. Introduction

Amphotericin B (AMB) is a drug widely used to treat systemic fungal infections and leishmaniasis [1,2]. These diseases are creating global health burdens due to significant morbidity and mortality in immune-compromised patients [3]. AMB is a high-molar-mass drug (Mw = 9.24×10^3 g/mol) and is composed of a hydrophobic polyethylene hydrocarbon chain and a hydrophilic polyhydroxylated side chain [4]. Due to its amphoteric nature, AMB presents low solubility in aqueous media and many organic solvents, leading to limited oral bioavailability (0.3%) and membrane permeability (log P 0.8); this makes it difficult to develop oral formulations, which is the most acceptable pathway of administration for the treatment of patients [1,4,5].

The benefits of AMB are impaired due to their high toxicity in normal tissues, leading to various side effects including infusion-related and chronic toxicity [6]. Amphotericin B toxicity is associated with the formation of aggregates in aqueous solutions [7], and to overcome this problem, new AMB formulations have been investigated. Fungizone® is a commercial drug to which a surfactant (sodium deoxycholate, DOC) is added to promote the dissolution of AMB in aqueous media; however, the DOC concentration used in Fungizone® is not sufficient to avoid AMB aggregation, leading to severe side effects and limiting its clinical applications [8,9].

The use of nanoparticles to treat parasitic diseases has proven to be effective [10]. Unlike traditional delivery devices, particles of small size (<1 μm) are more likely to accumulate at the site of action, increase the concentration of a drug at the target site, and hence improve therapeutic efficacy. Moreover, nanoparticles can protect drugs from chemical or enzymatic degradation. In previous studies in our laboratories, we examined biopolymer-based nanoparticles for the association and delivery of drugs of varying permeability (both Lipinsky and non-Lipinsky) and we obtained both in vitro and in vivo proofs-of-concept for their potential therapeutic efficacy [[11], [12], [13]]. Previous studies have attempted to produce novel AMB pharmaceutical formulations with lower toxicity and cheaper cost. Among these are novel polymeric nanocarriers [5,14] that can improve the stability of active substances. A cluster dextrin was evaluated for AMB encapsulation [15] and, although the system displayed self-aggregation as observed with Fungizone® and AmBiosome®, lower hemolytic activity and a higher retention of AMB in plasma was observed than with Fungizone® [15].

Many liposomal formulations have been developed and approved for use in the treatment of fungal infections, including AmBiosome® (amphotericin B-loaded liposomal), Amphotec® (AMB colloidal dispersion) and Abeltec® (AMB lipid complex) [15]. Even though these formulations decreased nephrotoxicity [16] unlike Fungizone®, they are expensive for the treatment of diseases such as Leishmaniasis, which is associated with malnutrition, displacement, poor housing, weak immune systems, and poverty.

Tiyaboonchai and Limpeanchob [17] produced a nanoformulation for AMB delivery by polyelectrolyte complexation of chitosan and dextran sulphate. This system showed aggregation patterns similar to those of Fungizone®, but its neurotoxicity was lower than that of the commercial formulation. The authors attributed this result to the slow release of AMB compared to that with Fungizone®.

Nanoemulsions containing cholesterol, with and without stearylamine (STE), were investigated for encapsulation of AMB [18]. The authors produced nanoemulsions with a size smaller than 200 nm, high AMB encapsulation, low cytotoxicity, and antileishmanial activity. Santos et al. [19] investigated the preparation of a nanoemulsion for encapsulation of AMB; the nanoemulsion was prepared with an oil phase composed of medium-chain triglycerides, Tween 80®, cholesterol, an antioxidant, and an aqueous phase composed of glycerol and purified water. Drop sizes ranging from 89 to 705 nm were produced, depending on homogeniser pressure and number of cycles. This AMB nanoemulsion showed a reduction in hemolytic activity, reduction in parasite burden, and absence of acute toxicity [19].

Recently, a Pickering emulsion stabilised by cashew gum-poly-lactide copolymer nanoparticles was reported, and this system is potentially useful to associate AMB into the Pickering emulsion in a less aggregated form than commercial AMB formulations [20]. To date, polysaccharide-based oil-core nanocapsules have not been evaluated either for the encapsulation of AMB, or the effect on the aggregation state of the drug, which are important considerations for future AMB therapies with reduced toxicity. Such systems are formed by spontaneous emulsification or solvent displacement [21,22].

In the present study, hydrophobic modification of Sterculia striata polysaccharide (SSP) was carried out and its derivatives characterised. The derivatives were used for production of stable nanocapsules

without the use of surfactant for emulsion stabilisation. As a proof-of-concept, the nanocapsules formed were tested as an encapsulation matrix for AMB, aiming to minimise its aggregation state, and for subsequent use as an AMB delivery platform with reduced toxicity. A comparison with commercial formulations was also undertaken.

Sterculia striata is a tree species belonging to the family Sterculiacea, popularly known in Brazil as 'chichá', and is widely found in the northeast and central regions of Brazil [23]. The exudate polysaccharide of this tree is very similar to Karaya gum, a commercial polysaccharide. The polysaccharide obtained from S. striata is a rhamnogalacturonoglycan, composed of uronic acid units (from 42.2 to 49.2%), rhamnose (23.8 to 28.8%), galactose (19.3 to 23.4%), xylose (5.6 to 7.7%), and acetyl groups (9.6%) [24,25]. Recent studies have used Sterculia striata polysaccharide (SSP) for the preparation of nanoparticles via complexation with chitosan and tested SSP as a potential chloroquine-incorporation matrix [26].

2. Experimental

2.1. Materials

Sterculia striata exudate was collected in Fortaleza, Ceará, Brazil. Purification was carried out as previously described [24]. Amphotericin B was supplied by Ethicall (Fortaleza, Brazil). Methanol and acetone were obtained from Synth (São Paulo, Brazil) and Miglyol812® from Cremer Oleo (Witten, Germany). All chemical reagents were used without further purification. A commercial solution of 250 μg/mL Amphotericin B (Sigma-Aldrich, São Paulo, Brazil) in deionised water, with sodium deoxycholate, was used for analysis of the AMB aggregation state. Sterculia striata polysaccharide (SSP) has been previously characterised and has a molar mass of 3.6×10^7 g/mol and monosaccharide molar ratios of uronic acid(galacturonic and glucuronic acids):rhamnose:galactose:xylose = 5.5:4.5:3.3:1.

2.2. Sterculia striata polysaccharide (SSP) acetylation

Modification of SSP was carried out according to the methodology proposed by Motozato, Ihara, Tomoda & Hirayama [27] with modifications. Sterculia striatapolysaccharide (0.5 g) was suspended in 20 mL of formamide at 50 °C, with vigorous stirring for 1 h. Pyridine (1.5 mL) and acetic

anhydride were added and the solution remained under magnetic stirring (100 rpm) for 24 h. The

acetylated SSP (ASSP) was precipitated by adding 400 mL of distilled water. The precipitate was

washed with distilled water and dried in hot air. Four ratios of monosaccharide unit:pyridine:acetic

anhydride were investigated (Table 1).

Table 1. Effect of reagent molar ratio on degree of substitution (DS) and yield.

Sample	Molar ratio M:P:Ac	% Acetyl groups	DS	Yield (%)
ASSP1	1:6:24	28.0 ± 0.8	1.68 ± 0.01	85 ± 2.5
ASSP2	1:6:12	24.0 ± 1.1	1.35 ± 0.01	63 ± 1.6
ASSP3	1:6:6	13.0 ± 1.0	0.84 ± 0.02	38 ± 3.7
ASSP4	1:3:6	8.0 ± 0.6	0.48 ± 0.01	35 ± 2.5

M:P:A = molar ratio of monosaccharide unit:pyridine:acetic anhydride.

2.3. Degree of substitution (DS)

The percentage of acetyl groups and the DS of acetylated samples were determined by the volumetric

method described by Sanchez-Rivera et al. [28]. Acetylated Sterculia striata polysaccharide (30 mg)

was weighed and transferred to a 250-mL flask and dispersed in 12 mL of NaOH 0.543 mol/L. The

flask was sealed and heated at 50 °C for 15 min and then placed for 72 h at room temperature, with

occasional stirring. Subsequently, the amount of unconsumed NaOH was determined by titration with

hydrochloric acid (HCl) 0.521 mol/L, using phenolphthalein as indicator. Determination of the acetyl

group was calculated with the following equation:

$$\text{Acetyl group}(\%) = \frac{(V1 - V2) \times M \times 0.043 \times 100}{w}$$

where V1 is the volume of 0.0521 mol/L HCl used to titrate the blank (mL), V2 is the volume of

0.0521 mol/L HCl used to titrate the sample (mL), M is the molarity of the HCl solution, and w is the

sample mass (g).

DS indicates the average number of hydroxyl groups substituted by acetyl groups per monosaccharide

unit, and was calculated as:

$$DS = \frac{181 \times Acetyl\ group\ (\%)}{4300 - 42 \times Acetyl\ group\ (\%)}$$

All analyses were performed in triplicate.

2.4. Nanocapsule preparations

Nanocapsules were prepared according to the protocol developed by Goycoolea et al. [11], with minor modifications. Briefly, the nanoemulsion was prepared by dissolving ASSP in 4.5 mL of acetone (ASSP concentrations in acetone: 0.5 and 1.0 mg/mL), 250 μL of methanol, and 62.5 μL of Miglyol812® (organic phase). This organic solution was then poured into 10 mL of deionised water (aqueous phase). Upon addition, the mixture immediately became milky due to the diffusion of acetone and methanol into the aqueous phase and the spontaneous formation of emulsified oil (Miglyol812®) nanodroplets. Finally, acetone, methanol, and a portion of the water were evaporated on a rotaevaporator at 40 °C, to reduce the final volume to one third of the original, yielding the aqueous suspension. After solvent evaporation, nanocapsules were isolated by centrifugation at 25,000 ×g (18,000 rpm) for 60 min. Nanocapsules were denominated NC1.68, NC1.35, NC0.84, and NC0.48, where the number after NC designates the DS of ASSP.

2.5. AMB incorporation and aggregation state

To encapsulate AMB, the same procedure for preparation of the nanocapsules described above was adopted, but with AMB being dissolved in a methanol aliquot (250 μL).

To investigate the effect of different AMB concentrations (0.25, 0.5, and 1.0 mg/mL in methanol) on drug encapsulation efficiency (EE%), nanocapsules were prepared using NC1.68 with an ASSP concentration of 1.0 mg/mL in acetone.

To investigate the effect of the degree of acetylation (NC1.68 and NC1.35) and ASSP concentration (0.5 and 1.0 mg/mL) on the AMB encapsulation efficiency, the AMB concentration was kept at 0.25 mg/mL.

The EE% and AMB aggregation state of the nanocapsules were determined using a Shimadzu UV-1800 UV–Visible spectrophotometer in the $\lambda = 250$ to 500 nm range. For determination of EE%, all

pellet volumes (nanocapsules extracted after centrifugation) were measured and methanol was added, at a methanol:pellet ratio of 2:1 (v/v). The samples were then centrifuged at 40,000 ×g for 30 min. The supernatants containing AMB were removed and analyzed on the UV–Vis spectrometer at 406 nm (Shimadzu UV 1800 spectrometer). The amount of encapsulated AMB was calculated using a calibration curve to determine the ratio of absorbance to concentration ($R^2 = 0.9969$). The following formula was used to calculate EE%:

$$EE\% = \frac{AMB \ mass \ in \ NC}{initial \ AMB \ add \ to \ NC} \times 100\%.$$

The state of aggregation of nanocapsules was determined before and after drug extraction. For the determination of the AMB aggregation state before the extraction, sample NC1.68 with different concentrations of AMB was used, being diluted to a final AMB concentration of 2×10^{-5} mol/L, and analyzed by UV–Vis. A nanocapsule without drug, diluted in deionised water, was used as the blank in this experiment. The Sigma AMB solution (with sodium deoxycholate) was diluted with deionised water to the same AMB concentration as in nanocapsules.

2.6. In vitro drug release

The release profiles of AMB loaded in NC 1.68 was obtained by dispersing the sample in HEPPES 10 mmol/L buffer with 0.25% sodium and introduce the dispersion into cellulose acetate membrane (cut off 14,000 g/mol). The dialyzed was carried out against 15 mL of HEPES buffer solution containing 0.25% sodium lauryl sulfate, at pH 7.4, and 37 °C for 225 h. Aliquots were taken at certain time intervals and analyzed by spectrophotometry in the UV–vis region. Absorbance measurements at 368 nm wavelength were converted into the percentage of drug released, according to a previously established calibration curve.

2.7. Hemolysis assay

To evaluated the toxicity of NC 1.68 loaded with AMB, its hemolytic activity was tested using human red blood cells (RBCs) was previously reported by Sahariah et al. [29]. Human blood was collected in EDTA tubes (1.8 mg/mL), washed three times and re-suspended with sterile saline solution (0.9%). The samples were tested at different AMB concentration, from 500 to 7.8 μg/mL. Triton X (0.1%) and

saline solution were used was positive and negative hemolysis control, respectively. The mixtures were incubated for 1 h at 37 °C and centrifuged at 10,000g for 1 min. After centrifugation time, the absorbance of samples supernatants was measured at 492 nm.

2.8. Morphology

Atomic force microscopy (AFM) was used to elucidate the structural characteristics of nanocapsules. NC 1.68 blank and AMB load were analyzed using a TT-AFM microscopy (AFM Workshop®, USA). The images were taken in tapping mode, using a silicon cantilevers (ACT20, APP NANO®) with the resonance frequency of approximately 365 kHz. 10 μL of diluted samples (1:1000 v/v) was spread onto freshly cleaned mica disks and dried for around 10 min at 40 °C. The images were processed using Gwyddion® 2.45 software.

2.9. In vitro antifungal assays — broth microdilution method

The minimum inhibitory concentration (MIC) of NC 1.68 and NC1.68 loaded with AMB against the yeast strains were determined by the broth microdilution method using 96-well plates according to the document M27-A3, from the Clinical and Laboratory Standards Institute-CLSI (formerly NCCLS) [30]. To 4.5 mL NC pellet, 0.150 mL of 0.25% sodium lauryl sulfate, was added to prepared the stock solution. From the stock solutions, both samples were serially diluted in RPMI 1640 medium, to cover a 0.007–16 μg/mL. AMB (0.007–16 μg/mL) was used as standard drug controls. The microplates were incubated at 35 °C and the fungal growth/inhibition observed after 48 h. The MIC was defined as the lowest concentration where no visual growth (no turbidity) was observed that corresponded to 90% inhibition of the fungus. Each experiment was performed in duplicate. The standard Candida albicans strain was obtained from the American Type Culture Collection (ATCC90028). Clinical isolates of C. albicans (n = 03) from Santa Casa de Misericórdia Hospital, Sobral (Ceará, Brazil), Fortaleza (Ceará, Brazil) (Table 3).

2.10. Infrared spectroscopy

The IR spectra of SSP and acetylated SSP were recorded in the solid state, using KBr pellets in a Bomem IR spectrometer (FTLA 2000) operating at wavenumber in the range 400–4000 cm−1.

2.11. Particle size and zeta potential

Sample particle sizes were measured on a NanoZeta Sizer (Malvern, ZS 3600) at 25 °C fitted with a red laser light output set at $\lambda = 632.8$ nm. The intensity size (hydrodynamic diameter) distributions were determined by dynamic light scattering with non-invasive back scattering (DLS-NIBS) and detection was done at an angle of 173°.

The zeta-potential was measured by phase analysis light scattering and mixed laser Doppler velocimetry (M3-PALS) at 25 °C, using the same instrument. For particle size and zeta-potential analysis, 50 µL of the nanocapsules were diluted in 950 µL of deionised water, and each sample was measured in triplicate.

2.12. Stability measurements

The storage stability of the isolated nanocapsules was determined by measuring the particle size and the polydispersive index of the nanocapsule alone, or with AMB, dispersed in distilled water according to time of storage. Samples were kept refrigerated at $4° \pm 2$ °C.

3. Results and discussion

3.1. Characterisation of acetylated Sterculia striata polysaccharide (ASSP)

The acetylated samples of ASSP, prepared by the addition of different volumes of acetic anhydride, were designated as ASSP1, ASSP2, ASSP3, and ASSP4. The molar ratio of monosaccharide unit:pyridine:acetic anhydride (M:P:A) used in this study is shown in Table 1. The DS indicates the average number of hydroxyl groups substituted by acetyl groups per monosaccharide unit. The increase in the P:A ratio (ASSP3 and ASSP4) did not affect the derivative yield; however, as an increase in DS was observed, we decided to investigate the concentration effect of anhydride, while keeping the M:P ratio constant (1:6). Increases in acetic anhydride concentrations produced increases in DS and yield (Table 1). A similar result was observed by Song et al. [31] for the acetylation of polysaccharides isolated from pumpkin, whereby the DS ranged from 0.41 to 0.67 with between one- and three-fold increases in the concentration of acetic anhydride triplicates.

The polysaccharide from Cyclocarya paliurus was acetylated with acetic anhydride and the DS values changed from 0.13 to 0.54 with between one and six fold increases in the concentration of acetic

anhydride [32]. Cashew gum was also acetylated with acetic anhydride and the DS value obtained was 2.8 [33].

The infrared spectra of SSP and acetylated derivatives (ASSP) are shown in Fig. 1. The SSP spectrum shows characteristic polysaccharide bands at 3500 cm−1 from the OH stretching vibration, as well as bands at 1150, 1080, and 1030 cm−1 due to COC stretching vibrations of glycosidic bonds and OH bending from alcohols. Sterculia striata polysaccharide also presents bands at 1612 and 1418 cm−1 due to the CO of the carboxylated groups of uronic acid in salt form, and CO and COC of acetyl groups at 1734 and 1231 cm−1, respectively [24].
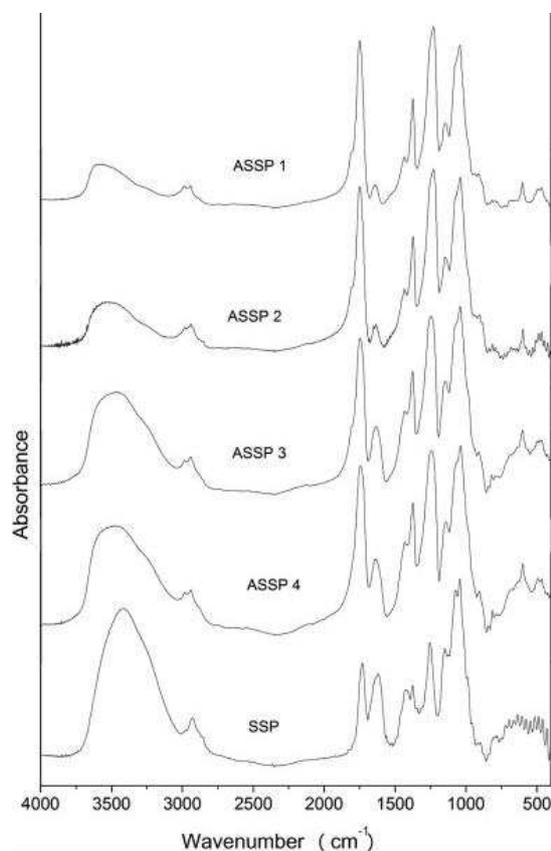
Fig. 1. FTIR spectra of SSP and acetylated derivatives. ASSP1 (DS 1.68), ASSP2 (DS 1.35), ASSP3 (DS 0.84), and ASSP4 (DS 0.68) in KBr.

The ASSP spectrum shows an increase in band intensity due to CO and COC of acetyl groups and concomitant decrease of the band at 3500 cm−1 due to substitution of hydroxyl groups that occur with

an increase of DS. As can be seen for ASSP 1.68, the lower intensity of the hydroxyl bands than the COC bands corroborates the assumption that DS 1.68 is almost the maximum that can be obtained for this polysaccharide.

3.2. Nanocapsule (NC) preparation and characterisation

To investigate the suitability of ASSP to stabilise the oil-in-water emulsion formed by solvent displacement, we evaluated the physical characteristics (average diameter, polydispersity, and zeta potential) of the formed nanocapsules. The nanocapsules were formed at two ASSP concentrations in the organic phase, namely 0.5 and 1.0 mg/mL. Interestingly, only ASSP samples with DS 1.68 (NC1.68) and 1.35 (NC1.35) formed a stable milky solution and a pellet after centrifuging, both characteristic hallmarks of the formation of a nanoemulsion [11].

Significantly, the nanocapsules of ASSP were formed without the use of any surfactant, in contrast with the original protocol for the preparation of chitosan-coated nanocapsules [21]. Variations of this original system have been reported, using polysaccharide or its derivatives. However, such studies generally report the use of surfactants such as lectin, Tween 20®, Spam80®, and dodecyltrimethylammonium chloride (DTAC) [11,22,34].

The effect of derivative DS as well as the concentration of ASSP in organic phase on the Z-average size is shown in Fig. 2A. At a low polysaccharide concentration (0.5 mg/mL), NC1.35 has a higher Z-average diameter (d = 245.5 ± 1.7 nm) than NC1.68 (d = 228.1 ± 2.5 nm); this high value may be attributed to a greater swelling of the less hydrophobic derivative. As the concentration increased to 1 mg/mL, NC1.68 presented a Z-average size higher (d = 273.9 ± 1.3 nm) than NC1.35 (d = 241.8 ± 1.2 nm). This may be because, as the concentration of ASSP increases, the inner oil phase increases more significantly for the derivative with a higher degree of substitution (DS 1.68), and the swelling of NC1.35 is not enough to overcome the increase in oil phase size in NC1.68. Fig. 2A shows that, for NC1.68, an increase in the ASSP concentration from 0.5 to 1.0 mg/mL led to an increase in Z-average size (228.1 ± 2.5 nm to 273.9 ± 1.3 nm), which may be due to an increase in the oil core as the concentration of hydrophobic derivatives increase, as previously proposed. In contrast, a different behaviour was observed for NC1.35, where the Z-average diameter is practically constant with increasing ASSP concentrations. We reasoned that, as the DS is smaller than that in NC1.68, the increased concentration of a hydrophobic derivative will modify the size of the oil core; however, it

may also produce less swelling of the hydrophilic layer, leading to a small decrease in size which has a more significant effect on NC1.35 than on NC1.68.
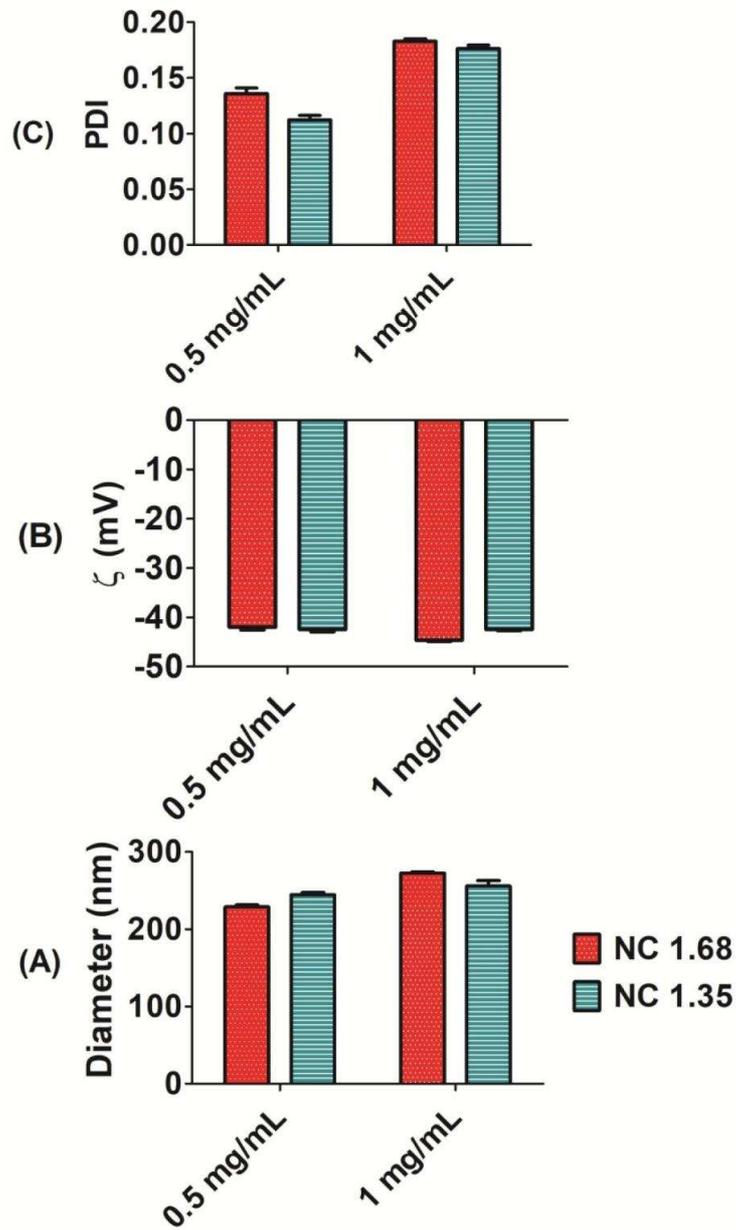
Fig. 2. Effect of Sterculia striata polysaccharide concentration on polydispersity, ζ-potential, and mean Z-values of nanocapsules.

Significantly, the Z-average size of ASSP nanocapsules is greater than in other systems based on

polysaccharides, such as chitosan [11,35]. Goycoolea et al. [11] using the same methodology, obtained nanoparticles with a Z-average size in the 127–219 nm range, which was dependent on chitosan molar mass (ranging from 9.6 to 266×103 g/mol) and degree of acetylation. Larger particles were observed by the authors when a high chitosan molar mass was used. The molar mass of SSP is very large (3.6×107 g/mol) in comparison to that of chitosan used in those experiments, implying that the increase in particle size of NC is due to the high molar mass of SSP.

As previously mentioned, Santos et al. [19] used a nanoemulsion with cholesterol to encapsulate AMB. No significant difference in size was observed after AMB encapsulation, and the optimised emulsion showed a size range between 136 ± 5 and 148 ± 2 nm for blank and loaded nanoemulsions, respectively [19].

Larabi et al. [36] produced a phospholipid emulsion to encapsulate AMB. The size ranged from 690 to 275 nm and all the conditions investigated were polydisperse and bimodal, and the addition of AMB increased the particle size. Caldeira et al. [18] produced nanoemulsions with a particle size smaller than 200 nm but, in these preparations, surfactants and ultra-turax with 8000 rpm were used.

Fig. 2B shows the ζ-potential for isolated NCs at 0.5 and 1 mg/mL ASSP concentrations. Data for the ζ-potential of isolated nanocapsules are similar for NCs prepared with ASSP with different DS, even at different derivative concentrations. The negative values (approximately -40 mV) indicate that the carboxylate groups of SSP are preferentially adsorbed at the nanocapsule surfaces due to the presence of uronic acid in salt form. Moreover, the large ζ values are characteristic of stable emulsion systems.

The polydispersity index (PDI) values (Fig. 2C) are smaller for NCs prepared at a lower concentration (PDI ~ 0.112 for NC1.35 and PDI ~ 0.130 for NC1.68) of ASSP than at 1 mg/mL (PDI ~ 0.177 for NC1.35 and PDI ~ 0.187 for NC1.68). The PDI values are in agreement with those of low polydispersed systems.

The effect of AMB incorporation on polydispersity, ζ-potential, and Z-average size for isolated NC1.68 and NC1.35 at 1 mg/mL ASSP concentration was also investigated. Incorporation of AMB into NC1.68 did not affect the Z-average size, polydispersity, or ζ-potential values (d $= 274.1 \pm 8.6$ nm; $\zeta = -39.8 \pm 0.2$ mV and PDI $= 0.181$). However, when NC1.35 was used, the particle size changed from 241.8 ± 1.2 nm to 277.3 ± 9.5 nm, and a decrease in the PDI value from 0.177 to 0.149 was observed; the particle size of NC1.68 may be enough to accommodate the AMB in the hydrophobic core without a significant change in size. For the less hydrophobic sample, however, an increase in particle size was

observed with incorporation of AMB. After incorporation, the sizes of both NC1.68 and NC1.35 were very similar.

Storage stability was investigated by measuring Z-average size and the polydispersity of NC1.68, with and without AMB, immediately after preparation, at 24 h, and at 1 year, using emulsion storage at 4 °C (Fig. 3).
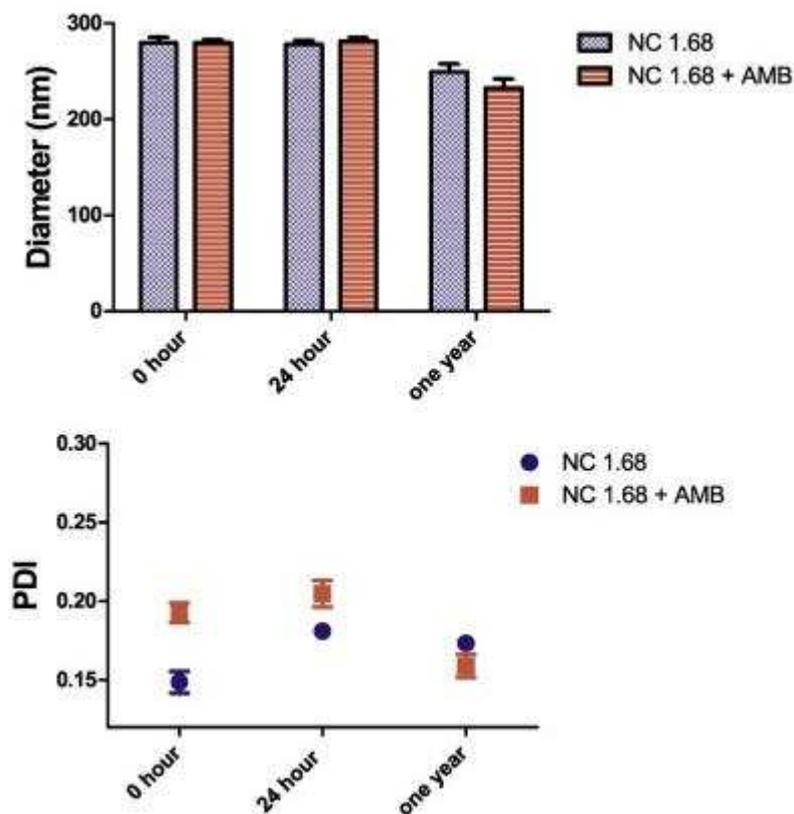
Fig. 3. Effect of time on particle size of the nanocapsules during storage in aqueous medium at 4 °C.

Fig. 3 shows that after the first 24 h, no significant decrease in size was observed either for empty or AMB loaded NC; after one year, storage under refrigeration showed a decrease of approximately 10% of the size observed for the empty nanocapsules (NC1.68); and of 16% for loaded nanocapsules (NC1.68 + AMB). These storage times indicate that the nanocapsule swelling equilibrium process is modulated as a function of time and by the presence of the hydrophobic drug. The incorporation of

AMB leads to a lower size due to a decrease in swelling promoted by a more hydrophobic core. The surface morphology of the NC 1.68 blank and AMB loaded were studied using an atomic force microscopy (AFM) (Fig. 4). AFM images of the nanocapsules showed spherical appearance and smooth surface for both blank and loaded AMB. Same pattern was observed in chitosan and carrageenan nanoemulsions surface [2].
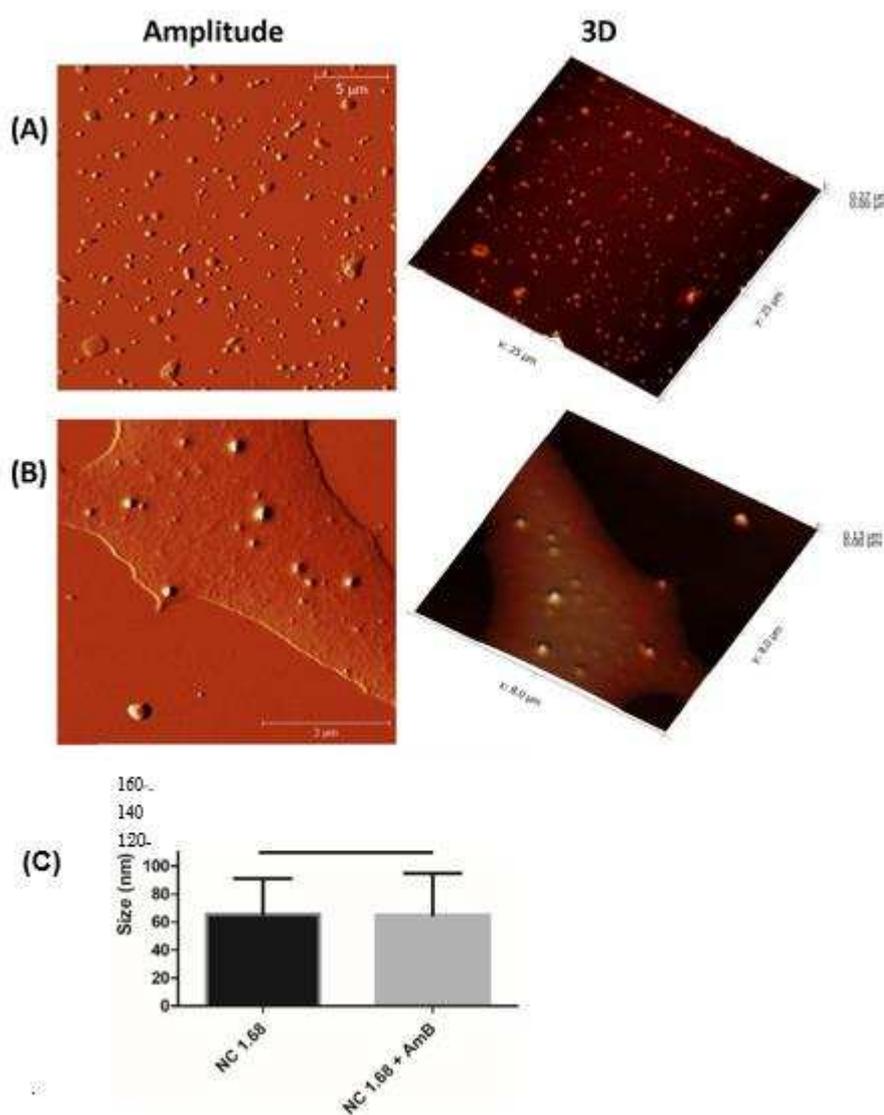
Fig. 4. AFM measurements of nanocapsules (a) NC 1.68 blank, (b) NC 1.68 loaded with AMB, and (c) average particles size estimated from the AFM images.

Nanoemulsion sizes by AFM for NC 1.68 + AMB were respectively 65.8 ± 25.5 nm for NC 1.68 and 65.0 ± 30.2 nm. The Student's t statistical test showed no statistical difference between blank or encapsulated AMB nanoemulsions. The size obtained is significantly smaller than that obtained by DLS, these differences may be due to the fact that AFM determines the diameter of the dry particles, and will probably cause them to shrink, whereas the DLS determines the hydrodynamic diameter in aqueous solution, which leads to swelling of the samples.

3.3. Analysis of AMB encapsulation efficiency and aggregation

The encapsulation efficiency (EE%) of AMB in NCs was determined using an initial AMB concentration of 0.25 mg/mL on NC preparation. High EE% values were obtained, ranging from 66.7 to 99.2% (Table 2). Almost all AMB was incorporated into NC1.68 (ASSP concentration of 1 mg/mL), the most hydrophobic matrix. As depicted in Table 2, a low ASSP DS and lower ASSP concentration lead to low AMB encapsulation. Tiyaboonchai and Limpeanchob [17] showed that the EE% ranged from 56 to 75%, depending on the chitosan:dextran sulphate ratio in the nanoparticles. Hydrophobised cluster dextrin presented an EE% varying from 7.7 to 19.1%, depending on the type of hydrophobic group inserted into the cluster dextrin. The values obtained in our study are higher than previously-cited polysaccharide-based matrices tested for AMB incorporation.

Table 2. Effect of ASSP concentration and DS on encapsulation efficiency (EE%).

Nanocapsule formulation	Concentration of ASSP (mg/mL)	Initial AMB concentration (mg/mL)	Encapsulation efficiency (%)
NC1.68	0.5	0.25	76.4 ± 3.5
NC1.68	1.0	0.25	99.2 ± 1.3
NC1.35	0.5	0.25	66.7 ± 2.6
NC1.35	1.0	0.25	80.5 ± 1.6
NC1.68	1.0	0.5	92.5 ± 4.8
NC1.68	1.0	1.0	45.5 ± 5.3

The effect of an increase in AMB concentration on EE% was investigated using NC1.68 (1.0 mg/mL ASSP matrix). The data showed that EE% decreased from 92.5 to 45.5% when the AMB concentration increased from 0.5 to 1.0 mg/mL. It can also be seen from Table 2 that a high incorporation efficiency was observed both when a more hydrophobic sample was used (NC1.68) and when the concentration of ASSP was high in the organic phase.

As previously mentioned, several studies have investigated new matrices for AMB encapsulation, with the aim of reducing AMB toxicity. The aggregation and solubility of AMB depends on the solvent used [37,38], concentration [39,40], and surfactant [41,42].

Evaluation of the aggregated state is generally monitored using UV–Vis spectroscopy. The UV–Vis AMB spectrum in its monomeric form, e.g., when the drug is dissolved in 50% methanol, shows four bands in the range of 345 to 406 nm. The band at 406 nm is characteristic of the monomeric form and the band at 345 nm is attributable to the aggregated form of AMB. The A345/A406 ratio for AMB in its monomeric form is approximately 0.3, while in its aggregated form it is higher than 2 [[43], [44], [45]].

Commercial AMB formulations such as Amphocil®, Fungizone®, Abeltec®, and AmBisome® were found to be in the aggregated form (in 5% dextrose), with A345/A406 ratios of 9.1, 4.8, 1.3, and 2.9, respectively [46].

Do Egito et al. [40] investigated the effect of AMB nanoemulsion on its aggregation pattern. It was shown that commercial AMB and Fungizone® solutions (both using DOC as surfactant) aggregated in AMB aqueous solutions above 5×10^{-7} mol/L and the AMB nanoemulsion produced did not prevent AMB aggregation, even at very low AMB concentrations such as at 5×10^{-8} mol/L. Chitosan-dextran sulphate and hydrophobised cluster dextrin nanoparticles with cholesterol also did not prevent AMB aggregation [15,17].

The UV–Vis spectra of AMB incorporated into NC1.68 at an ASSP concentration of 1 mg/mL, of NC1.68 (without drug), and commercial AMB aqueous solutions at an AMB concentration of 2×10^{-5} mol/L were recorded, using unloaded NC as a blank (Fig. 5). The commercial AMB solution shows four bands at 407, 384, 363, and 326 nm, the latter band being characteristic of AMB in the aggregated state, whereas the band at 407 nm was assigned to monomeric AMB. Similar bands were obtained for methanol, except for the band of aggregated AMB, which appears at 346 nm.
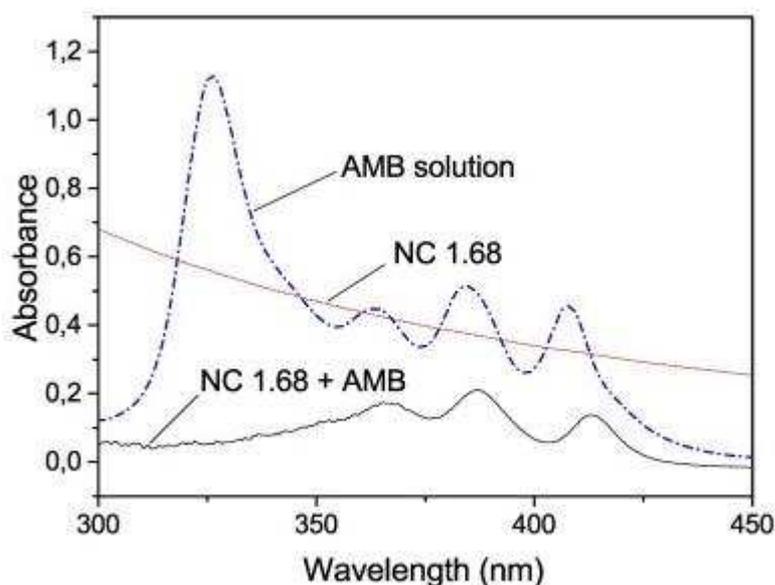
Fig. 5. UV–Vis spectra of AMB incorporated into NC1.68 and commercial AMB solution (Sigma-Aldrich) in aqueous solution at the AMB concentration of 2×10^{-5} mol/L.

The NC1.68 AMB spectrum exhibits shifts in the monomeric and aggregate bands at 413, 387, 365, and 326 nm. Changes in maximum absorption were reported as being dependent on the state of aggregation, as well as the medium used (406–420; 385–383; 363–360, and 345–328 nm) [5]. The ratio of aggregated to monomeric AMB bands (A326/A413) was found to be 0.37 for NC1.68 AMB and 2.47 for the AMB Sigma commercial solution. In this experiment, the concentration of AMB for both systems was 2×10^{-5} mol/L, one hundredfold more concentrated than that reported for a monomeric AMB solution [40].

Interestingly, it is known that the monomeric form of AMB influences drug toxicity. Nishi et al. [47] reported a similar behaviour for the Arabic gum-amphotericin B conjugate system, with AMB in its monomeric state (415 nm). Caldeira et al. [18] also reported that AMB nanoemulsions composed of cholesterol, with and without stearylamine, showed UV–Vis spectra where the bands referring to AMB association (327–340 nm) were reduced in comparison with the band for AMB in monomeric form. As a consequence, the oil-core nanocapsules were reported to encapsulate monomeric AMB.

To the best of our knowledge, this is the first time that nanocapsules based on a polysaccharide derivative is reported to reduce AMB aggregation. Importantly, these nanocapsules were produced spontaneously by mixing the oil and the aqueous phases without the use of a surfactant for emulsion

stabilisation.

In order to investigate the potential of NC1.68 sample as AMB drug delivery device, an in vitro release experiment was carried out using HEPPES 10 mmol/L buffer with 0.25% sodium lauryl sulfate as release medium. The in vitro release profile of AMB from NC 1.68 was show in Fig. 6. The profile shows a sustained drug release, with initial AMB released of $3.6 \pm 0.5\%$ after 1 h and of $49.1 \pm 0.4\%$ after 72 h. Complete release was observed after 212 h. This slow release may be due to the strong interaction of the AMB with the matrix, which hinders the drug exit to the medium and can be evidenced by the high encapsulation efficiency of 99.2%. AMB loaded polycarbonate micelles shows $48.6 \pm 2.1\%$ and $59.2 \pm 1.8\%$ of the AMB loaded released in 24 h [48].
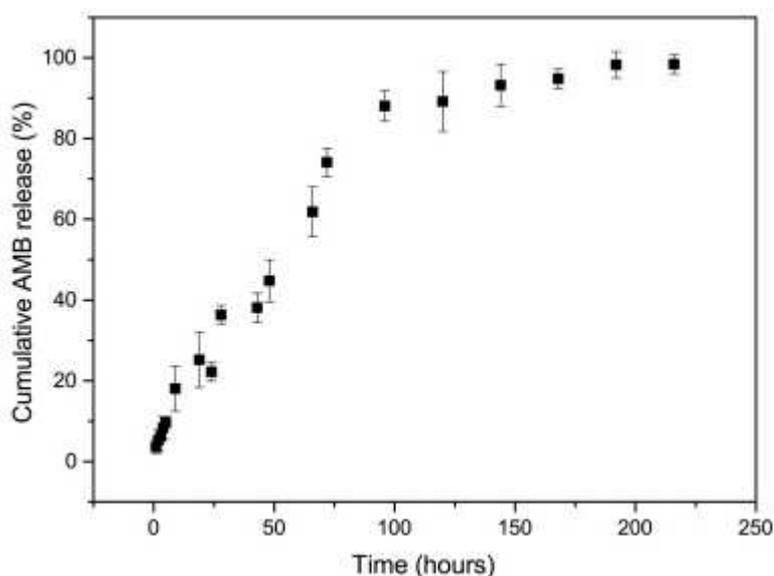
Fig. 6. In vitro release of AMB from NC 1.68 nanocapsules in HEPPES 10 mmol/L buffer with 0.25% sodium lauryl sulfate buffer, pH = 7.4 at 37 °C.

Several kinetic models have been used to evaluate drug release in nanocarriers systems, the best fit (R = 0.996) for the system NC1.68 loaded AMB was the Higuchi model.

$$Q_t/Q_0 = K \times t^{1/2}$$

where Qt is the amount of AMB release in time t, K is the release constant, and t is the time. This kinetic model shows that a drug homogeneously dispersed and dissolved in a polymer matrix tends to diffuse through the membrane [50].

3.4. Biocompatibility assessment

Fig. 7 show the results of hemolysis experiments to NC 1.68 blank and AMB loaded. Incubation of RBCs with triton X (0.1%), as a positive control, led to lysis in red cells instantly, causing 100% hemolysis and releasing hemoglobin, which causes the solution to become cloudy after centrifugation, saline solution (0.9%) was used as negative control.
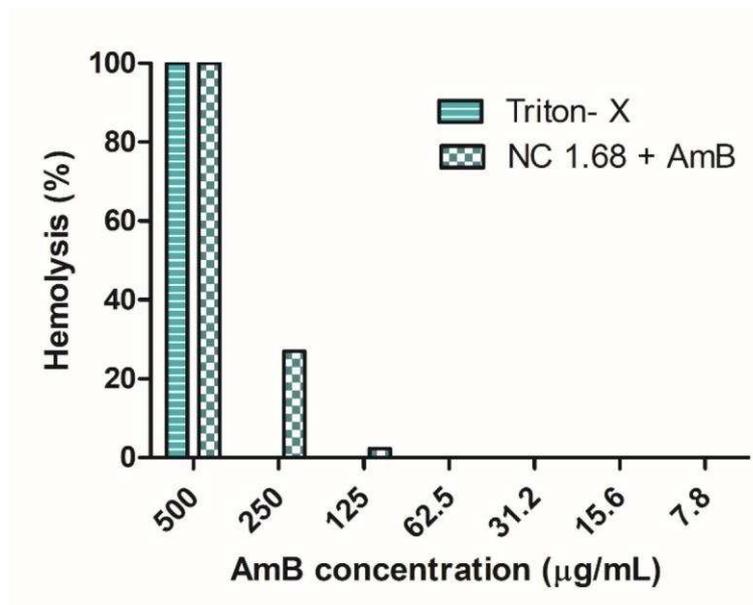
Fig. 7. Bar diagram of % of hemolysis as a function of AMB concentration for NC 1.68 + AMB. Triton was used as a positive control.

NC 1.68 + AMB exhibit good compatibility with erythroses. A low percentage of hemolysis was observed only when the AMB concentration was 125 μg/mL (2.3 ± 0.4%). However at concentration as high as 500 μg/mL NC 1.68 + AMB sample promote a 100% lysis.

Larabi et al. [49] tested the hemolytic activity for pure AMB in DMSO solution, and caused 50% at

concentration of 3.5 μg/mL. Kaneo et al. [5] tested AMB and Fungizone® at RBCs from male mice in PBS Buffer, pH 7.4. Alone AMB caused 100% hemolysis at concentration >8 μg/mL and Fungizone® caused 50% hemolysis at concentration 10.5 μg/mL.

Chitosan functionalized nanoparticles were tested at concentration of 12.5 and 25 μg/mL AMB by 6, 24 and 48 h. The nanoparticles presented negligible disruption of blood cells (<10%) independent of concentration or time [50]. Sulfonated chitosan nanoparticles caused <5% hemolysis for the range (20 to 80 μg/mL) of AMB tested [51]. Cluster dextrin nanoparticles hydrophobized whit cholesterol were completely non-hemolytic up to 30 μg/mL [15].

Comparison of results obtained by this study with the reported above shows that NC 1.68 AMB loaded nanocapsules exerts a stabilizing and protective effect on the cells against hemolysis even at higher AMB concentration than the previously reported systems.

3.5. In vitro antifungal test

NC1.68 and AMB loaded NC 1.68 antifungal susceptibility tests were carried out. The MICs of against five strains of C. albicans are summarized in Table 3, as well as the MICs of the current drug AMB. NC 1.68 sample does not show any activity against C. albicans, however AMB loaded NC 1.68 has the same MIC than standard drug control (AMB solution from Sigma-Aldrich).

Table 3. Determination of the minimum inhibitory concentration (MIC) of the AMB loaded and unloaded NC 1.68 against Candida albicans strains.

C. albicans strains	Source	MIC (μg/mL)		
		NC 1.68	AMB loaded NC 1.68	AMB (Sigma-Aldrich)
ATCC 90028	Culture collection	N.I	0.25	0.25
LABMIC 0104	Tracheal aspirate	N.I	0.25	0.25
LABMIC 0105	Hemoculture	N.I	0.25	0.25
LABMIC 0106	Urine	N.I	0.25	0.25

Sosa et al. [52] investigated nanoemulsion made with different oil and surfactants as drug delivery system of AMB for skin treatment against Candida ssp. and Aspergillus ssp. The authors shows that the MIC values for AMB loaded nanoemulsion was slightly greater (ranging to 0.38 to 0.78 μg/mL for Candida ssp.) than the free AMB (0.10 μg/mL).

4. Conclusion

Acetylated Sterculia striata polysaccharide (ASSP) derivatives with four different degrees of substitution (DS) were synthesised and characterised. The derivatives with high DS (1.66 and 1.35) produced stable oil-core nanocapsules without the use of a surfactant. Size distribution profiles are monomodal and no aggregation was observed, even one year after amphotericin B (AMB) encapsulation. The encapsulation efficiency (EE%) was as high as 99.2% in aqueous medium, and was found to depend on ASSP degree of substitution and concentration, as well as on drug concentration, and AMB was always found in a monomeric state. Nanocapsules of ASSP loaded with AMB (AMB loaded NC 1.68) shows good hemocompatibility, antifungal activity and a release control of drug up to 212 h. The results indicate that ASSP derivative in an oil-core nanocapsule is a potential candidate as an AMB delivery system.

References

[1] A.E. Silva, G. Barratt, M. Chéron, E.S.T. Egito

Development of oil-in-water microemulsions for the oral delivery of amphotericin B

Int. J. Pharm., 454 (2013), pp. 641-648, 10.1016/j.ijpharm.2013.05.044

 [2] A. Halperin, Y. Shadkchan, E. Pisarevsky, A.M. Szpilman, H. Sandovsky, N. Osherov, I. Benhar

Novel water-soluble amphotericin B-PEG conjugates with low toxicity and potent in vivo efficacy

J. Med. Chem., 59 (2016), pp. 1197-1206, 10.1021/acs.jmedchem.5b01862

 [3] S. Ravikumar, M.S. Win, L.Y.A. Chai Optimizing outcomes in immunocompromised hosts:

understanding the role of immunotherapy in invasive fungal diseases Front. Microbiol., 6 (2015), pp.

1-10, 10.3389/fmicb.2015.01322

 [4] B.T. Al-quadeib, M.A. Radwan, L. Siller, B. Horrocks, M.C. Wright

Stealth amphotericin B nanoparticles for oral drug delivery: in vitro optimization

Saudi Pharm. J., 23 (2015), pp. 290-302, 10.1016/j.jsps.2014.11.004

 [5] J.J. Torrado, R. Espada, M.P. Ballesteros, S. Torrado-Santiago

Amphotericin B formulation and drug targeting J. Pharm. Sci., 97 (2008), pp. 2405-2425,

10.1002/jps.21179

 [6] D.M. Casa, T.C. Carraro, L.E. Camargo, L.F. Dalmolin, N.M. Khalil, R.M. Mainardes

Poly(l-lactide) nanoparticles reduce amphotericin B cytotoxicity and maintain its in vitro antifungal

activity J. Nanosci. Nanotechnol., 15 (2015), pp. 848-854

 [7] Y. Wang, X. Ke, Z.X. Voo, S.S.L. Yap, C. Yang, S. Gao, S.S. Liu, S. Venkataraman, A.A.O.

Obuobi, J.S. Khara, Y.Y. Yang Biodegradable functional polycarbonate micelles for controlled release

of amphotericin B

Acta Biomater., 46 (2016), pp. 211-220, 10.1016/j.actbio.2016.09.036

  [8] G. Barratt, S. Bretagne Optimizing efficacy of Amphotericin B through nanomodification

Int. J. Nanomedicine, 2 (2007), pp. 301-313

 [9] R. Laniado-Laborin, M.N. Cabrales-Vargas Amphotericin B: side effects and toxicity

Rev. Iberoam. Micol., 26 (2009), pp. 223-227, 10.1016/j.riam.2009.06.003

 [10] A.M. Binnebose, S.L. Haughney, R. Martin, P.M. Imerman, B. Narasimhan, B.H. Bellaire

Polyanhydride nanoparticle delivery platform dramatically enhances killing of filarial worms

PLoS Negl. Trop. Dis., 9 (2015), pp. 1-18, 10.1371/journal.pntd.0004173

[11] F.M. Goycoolea, A. Valle-Gallego, R. Stefani, B. Menchicchi, L. David, C. Rochas, M.J. Santander-ortega, M.J. Alonso Chitosan-based nanocapsules: physical characterization, stability in biological media and capsaicin encapsulation. Colloid Polym. Sci., 290 (2012), pp. 1423-1434, 10.1007/s00396-012-2669-z

[12] F.M. Goycoolea, G. Lollo, C. Remuñán-López, F. Quaglia, M.J. Alonso

Chitosan-alginate blended nanoparticles as carriers for the transmucosal delivery of macromolecules

Biomacromolecules, 10 (2009), pp. 1736-1743, 10.1021/bm9001377

[13] S. Pistone, F.M. Goycoolea, A. Young, G. Smistad, M. Hiorth Formulation of polysaccharide-based nanoparticles for local administration into the oral cavity

Eur. J. Pharm. Sci., 96 (2017), pp. 381-389, 10.1016/j.ejps.2016.10.012

[14] N. Durán, P.D. Marcato, Z. Teixeira, M. Durán, F.T.M. Costa, M. Brocchi

State of the art of nanobiotechnology applications in neglected diseases

Curr. Nanosci., 5 (2009), pp. 396-408, 10.2174/157341309789378069

[15] Y. Kaneo, K. Taguchi, T. Tanaka, S. Yamamoto Nanoparticles of hydrophobized cluster dextrin as biodegradable drug carriers: solubilization and encapsulation of amphotericin B

J. Drug Deliv. Sci. Technol., 24 (2014), pp. 344-351, 10.1016/S1773-2247(14)50072-X

[16] G. Boswell, D. Buell, I. Bekersky AmBisome (liposomal amphotericin B): a comparative review

J. Clin. Pharmacol., 38 (1998), pp. 583-592

[17] W. Tiyaboonchai, N. Limpeanchob. Formulation and characterization of amphotericin B-chitosan-dextran sulfate nanoparticles. Int. J. Pharm., 329 (2007), pp. 142-149, 10.1016/j.ijpharm.2006.08.013

[18] L.R. Caldeira, F.R. Fernandes, D.F. Costa, F. Frézard, L.C.C. Afonso, L.A.M. Ferreira

Nanoemulsions loaded with amphotericin B: a new approach for the treatment of leishmaniasis

Eur. J. Pharm. Sci., 70 (2015), pp. 125-131, 10.1016/j.ejps.2015.01.015

[19] D.C.M.D. Santos, M.L.S. de Souza, E.M. Teixeira, L.L. Alves, J.M.C. Vilela, M. Andrade, M.D.G. Carvalho, A.P. Fernandes, L.A.M. Ferreira, M.M.G. Aguiar

A new formulation improves antileishmanial activity and reduces toxicity of amphotericin B

J. Drug Target., 26 (2017), pp. 357-364, 10.1080/1061186X.2017.1387787

[20] A.R. Richter, J.P.A. Feitosa, H.C.B. Paula, F.M. Goycolea, R.C.M. de Paula

Pickering emulsion stabilized by cashew gum-poly-l-lactide copolymer nanoparticles: synthesis,

characterization and amphotericin B encapsulation. Colloids Surf. B: Biointerfaces, 164 (2018), pp.

201-209, 10.1016/j.colsurfb.2018.01.023

[21] P. Calvo, C. Remunan-Lopez. Development of positively charged colloidal drug carriers:

chitosan-coated polyester nanocapsules and submicron-emulsions. Colloid Polym. Sci., 275 (1997), pp.

46-53

[22] A. Rosas-Durazo, J. Lizardi, I. Higuera-Ciapara, W. Argüelles-Monal, F.M. Goycoolea

Development and characterization of nanocapsules comprising dodecyltrimethylammonium chloride

and κ-carrageenan. Colloids Surf. B: Biointerfaces, 86 (2011), pp. 242-246,

10.1016/j.colsurfb.2011.03.020

[23] M.B.P. Mangas, V.M. Mello, P.A.Z. Suarez Thermal behavior of Sterculia striata oil

Thermochim. Acta, 564 (2013), pp. 39-42, 10.1016/j.tca.2013.03.035

[24] A.C.F. Brito, D.A. Silva, R.C.M. de Paula, J.P.A. Feitosa

Sterculia striata exudate polysaccharide: characterization, rheological properties and comparison with

Sterculia urens (karaya) polysaccharide. Polym. Int., 53 (2004), pp. 1025-1032, 10.1002/pi.1468

[25] A.C.F. De Brito, M.R. Sierakowski, F. Reicher, J.P.A. Feitosa, R.C.M. de Paula

Dynamic rheological study of Sterculia striata and karaya polysaccharides in aqueous solution

Food Hydrocoll., 19 (2005), pp. 861-867, 10.1016/j.foodhyd.2004.10.035

[26]G.A. Magalhães, E. Moura Neto, V.G. Sombra, A.R. Richter, C.M.W.S. Abreu, J.P.A. Feitosa,

H.C.B. Paula, F.M. Goycoolea, R.C.M. de Paula

Chitosan/Sterculia striata polysaccharides nanocomplex as a potential chloroquine drug release device

Int. J. Biol. Macromol., 88 (2016) (2016), pp. 244-253, 10.1016/j.ijbiomac.2016.03.070

[27] Y. Motozato, H. Ihara, T. Tomoda, C. Hirayama

Preparation and gel permeation chromatographic properties of pullulan spheres

J. Chromatogr. A, 355 (1986) (1986), pp. 434-437, 10.1016/S0021-9673(01)97349-2

[28] M.M. Sanchez-Rivera, I. Flores-Ramírez, P.B. Zamudio-Flores, R.A. González-Soto, S.L.

Rodríguez-Ambríz, L.A. Bello-Pérez. Acetylation of banana (Musa paradisiaca L.) and maize (Zea

mays L.) starches using a microwave heating procedure and iodine as catalyst: partial characterization

Starch/Staerke, 6 (2010), pp. 155-164, 10.1016/j.carbpol.2012.10.040

[29] P. Sahariah, B.E. Benediktssdóttir, M.A. Hjálmarsdóttir, O.E. Sigurjonsson, K.K. Sørensen, M.B. Thygesen, K.J. Jensen, M. Másson. Impact of chain length on antibacterial activity and hemocompatibility of quaternary N-alkyl and N,N-dialkyl chitosan derivatives

Biomacromolecules, 16 (2015), pp. 1449-1460, 10.1021/acs.biomac.5b00163

[30] Clinical and Laboratory Standards Institute. Reference Method for Broth Dilution Antifungal Susceptibility Testing of Yeast. Third Edition: Approved Standard M27-A3

CLSI, Wayne, PA, USA (2008)

[31] Y. Song, Y. Yang, Y. Zhang, L. Duan, C. Zhou, Y. Ni, X. Liao, Q. Li, X. Hu

Effect of acetylation on antioxidant and cytoprotective activity of polysaccharides isolated from pumpkin (Cucurbita pepo, lady godiva) Carbohydr. Polym., 98 (2013), pp. 686-691, 10.1016/j.carbpol.2013.06.049

[32] J.H. Xie, F. Zhang, Z.J. Wang, M.Y. Shen, S.P. Nie, M.Y. Xie

Preparation, characterization and antioxidant activities of acetylated polysaccharides from Cyclocarya paliurus leaves. Carbohydr. Polym., 133 (2015), pp. 596-604, 10.1016/j.carbpol.2015.07.031

[33] N.A.O. Pitombeira, J.G. Veras Neto, D.A. Silva, J.P.A. Feitosa, H.C.B. Paula, R.C.M. De Paula

Self-assembled nanoparticles of acetylated cashew gum: characterization and evaluation as potential drug carrier. Carbohydr. Polym., 117 (2015), pp. 610-615, 10.1016/j.carbpol.2014.09.087

[34] M. Artiga-Artigas, A. Acevedo-Fani, O. Martín-Belloso

Effect of sodium alginate incorporation procedure on the physicochemical properties of nanoemulsions Food Hydrocoll., 70 (2017), pp. 191-200, 10.1016/j.foodhyd.2017.04.006

[35] M.V. Lozano, D. Torrecilla, D. Torres, A. Vidal, F. Domínguez, M.J. Alonso

Highly efficient system to deliver taxanes into tumor cells: docetaxel-loaded chitosan oligomer colloidal carriers. Biomacromolecules, 9 (2008), pp. 2186-2193, 10.1021/bm800298u

CrossRefView Record in ScopusGoogle Scholar

[36] M. Larabi, N. Pages, F. Pons, M. Appel, A. Gulik, J. Schlatter, S. Bouvet, G. Barratt

Study of the toxicity of a new lipid complex formulation of amphotericin B

J. Antimicrob. Chemother., 53 (2004), pp. 81-88, 10.1093/jac/dkh025

[37] I. Gruda, N. Dussault. Effect of the aggregation state of amphotericin B on its interaction with ergosterol. Biochem. Cell Biol., 66 (1988), pp. 177-183

[38] J. Mazerski, J. Grzybowska, E. Borowski

Influence of net charge on the aggregation and solubility behaviour of amphotericin B and its

derivatives in aqueous media Eur. Biophys. J., 18 (1990), pp. 159-164

[39] P. Legrand, E.A. Romero, B.E. Cohen, J. Bolard

Effects of aggregation and solvent on the toxicity of amphotericin B to human erythrocytes

Antimicrob. Agents Chemother., 36 (1992), pp. 2518-2522

[40] E.S.T. Do Egito, H. Fessi, M. Appel, G. Barratt, P. Legrand, J. Bolard, J-Ph. Devissaguet

A morphological study of an amphotericin B emulsion-based delivery system

Int. J. Pharm., 145 (1996), pp. 17-27, 10.1016/S0378-5173(96)04713-8

[41] M.S. Espuelas, P. Legrand, M. Cheron, G. Barratt, F. Puisieux, J.-Ph. Devissaguet, J.M. Irache

Interaction of amphotericin B with polymeric colloids a spectroscopic study

Colloids Surf. B: Biointerfaces., 11 (1998), pp. 141-151, 10.1016/S0927-7765(98)00033-2

[42] P. Tancrède, J. Barwicz, S. Jutras, I. Gruda The effect of surfactants on the aggregation state of

amphotericin B. Biochim. Biophys. Acta, 1030 (1990), pp. 289-295, 10.1016/0005-2736(90)90305-8

[43] K. Gilani, E. Moazeni, T. Ramezanli, M. Amini, M.R. Fazeli, H. Jamalifar

Development of respirable nanomicelle carriers for delivery of amphotericin B by jet nebulization

J. Pharm. Sci., 100 (2011), pp. 252-259, 10.1002/jps.22274

[44] M.L. Adams, D.R. Andes, G.S. Kwon. Amphotericin B encapsulated in micelles based on

poly(ethylene oxide)-block-poly(l-amino acid) derivatives exerts reduced in vitro hemolysis but

maintains potent in vivo antifungal activity. Biomacromolecules, 4 (2003), pp. 750-757,

10.1021/bm0257614

[45] J. Barwicz, S. Christian, I. Gruda.Effects of aggregation of amphotericin B on its toxicity to mice

Antimicrob. Agents Chemother., 36 (1992), pp. 2310-2315

[46] A.B. Mullen, K.C. Carter, A.J. Baillie. Comparison of the efficacies of various formulations of

amphotericin B against murine visceral leishmaniasis. Antimicrob. Agents Chemother., 41 (1997), pp.

2089-2092

[47] K.K. Nishi, M. Antony, P.V. Mohanan, T.V. Anilkumar, P.M. Loiseau, P.M.;.A. Jayakrishnan

Amphotericin B–gum Arabic conjugates: synthesis, toxicity, bioavailability, and activities against

leishmania and fungi. Pharm. Res., 24 (2007), pp. 971-980, 10.1007/s11095-006-9222-z

[48] T. Higuchi Mechanism of sustained-action medication. Theoretical analysis of rate of release of solid drugs dispersed in solid matrices. J. Pharm. Sci., 52 (1963), pp. 1145-1149, 10.1002/jps.2600521210

[49] M. Larabi, V. Yardley, P.M. Loiseau, M. Appel, P. Legrand, A. Gulik, S.L. Croft, G. Barratt, C. Bories Toxicity and antileishmanial activity of a new stable lipid suspension of amphotericin B toxicity and antileishmanial activity of a new stable lipid suspension of amphotericin B

Antimicrob. Agents Chemother., 47 (2003), pp. 3774-3779, 10.1128/AAC.47.12.3774-3779.2003

[50] R.G. Vásquez Marcano, T.T. Tominaga, N.M. Khalil, L.S. Pedroso, R.M. Mainardes Chitosan functionalized poly(ε-caprolactone) nanoparticles for amphotericin B delivery

Carbohydr. Polym., 202 (2018), pp. 345-354, 10.1016/j.carbpol.2018.08.142

[51] M. Sandhya, V. Aparna, S. Maneesha, K.B. Raja, R. Jayakumar, S. Sathianarayanan Amphotericin B loaded sulfonated chitosan nanoparticles for targeting macrophages to treat intracellular Candida glabrata infections

Int. J. Biol. Macromol., 110 (2018), pp. 133-139, 10.1016/j.ijbiomac.2018.01.028

[52] L. Sosa, B. Clares, H.L. Alvarado, N. Bozal, O. Domenech, A.C. Calpena Amphotericin B releasing topical nanoemulsion for the treatment of candidiasis and aspergillosis

Nanomed. Nanotechnol., 13 (2017), pp. 2303-2312, 10.1016/j.nano.2017.06.021